Co@C,MnO-NAC Via Selectively Wrapping for Effective Oxygen Electrocatalysis in Rechargeable Zn-air Battery

Wenshu Zhou [a], Yanyan Liu [a, c, d], Dichao Wu [a], Pengxiang Zhang [d], Gaoyue Zhang [a], Kang Sun [a], Baojun Li [d], Jianchun Jiang [a, b,] *

[a] Institute of Chemical Industry of Forest Products, Chinese Academy of Forestry (CAF), National Engineering Lab. for Biomass Chemical Utilization, Key and Open Lab. of Forest Chemical Engineering, SFA, Nanjing, Jiangsu Province, 210042, China.

[b] Co-Innovation Center of Efficient Processing and Utilization of Forest Resources, Nanjing Forestry University, Nanjing, China.

[c] College of Science, Henan Agricultural University, Zhengzhou, China

[d] College of Chemistry and Molecular Engineering, Zhengzhou University, Zhengzhou, China

* Corresponding Author. E-mail: jiangjc@icifp.cn (J.C. Jiang)

Experimental section

Synthesis of activated carbon (AC)

The branches of broussonetia papyrifera, as the precursors, was pretreated by washing with ethanol and distilled water, and dried. The obtained clean branches of broussonetia papyrifera was cut into fragments and ground into powder. 20 g powder was dissolved in 2 M acetic acid (250 mL) and hydrothermal treatment at 180 °C for 30 hours. The obtained brown product was named as hydrothermal carbon (HC). Then, the HC were calcined at 600 °C under N_2 for 2 hours to obtain carbide carbon, named as CC-600. 1 g CC-600 mixed with 4 g of potassium hydroxide and annealed in a tube activation furnace at 900 °C for 2 hours under N_2 atmosphere. Finally, the obtained product was washed with hydrochloric acid (2 M) and deionized water until neutral, and dried at 120 °C for 24 hours to obtain the activated carbon (AC).

Synthesis of N-doped activated carbon (NAC)

AC (0.25 g) and melamine (1.25 g) were grounded homogeneously, then annealed in a tube furnace at 800 ºC for 2 hours in N_2 atmosphere to obtain nitrogen-doped activated carbon, denoted as NAC.

Synthesis of Co, MnO, N-codoped activated carbon (Co@C,MnO-NAC)

Mn(Ac)$_2$·4H$_2$O (0.246 g) and Co(Ac)$_2$·4H$_2$O (0.500 g) were dissolved in 50 mL of deionized water and sonicated for 15 min. NAC (0.3 g) was added into the above solution with stirring at 600 rpm. Then NH$_3$·H$_2$O (420 μL) was added by drop-wise, and kept at 60 °C for 6 hours. After that, the solution was transferred into autoclave for the hydrothermal reaction at 150 °C for 5 hours. The product was collected by filtration and dried at 80 °C for 24 hours. Then they were calcined at 750 °C for 2 hours under N$_2$ atmosphere to generate Co@C,MnO-NAC. MnO-NAC and Co@C-NAC was synthesized by the similar process without adding the Co(Ac)$_2$·4H$_2$O or Mn(Ac)$_2$·4H$_2$O, respectively.

Characterization

Transmission electron microscopy (TEM) images were collected from JEOL-JEM-2100 with elemental mappings collected by EDAX. The crystal structure of products were was identified by X-ray diffraction (XRD) using a Brüker D8 advance with Cu Kα radiation (λ= 1.5418 Å). Raman spectra was obtained on a Renishaw RM-1000 with Ar-ion laser (λ=514 nm). X-ray photoelectron spectroscopy (XPS) was investigated on the Thermo Scientific K-Alpha+ with Al Kα X-ray as the excitation source. N$_2$ sorption isotherms were measured on a urface area and porosity analyzer (Micrometrics Tristar 3020 s) at 77.35 K.

Electrochemical measurements

All the electrochemical tests were carried out on a CHI 760E electrochemical workstation (CH Instruments, Inc, Shanghai) equipped with a rotating ring-disk electrode (RRDE) system in a standard three-electrode system with KOH as the electrolyte a platinum wire as the counter electrode, Ag/AgCl electrode as the reference electrode and a modified glassy carbon electrode as the working electrode. All the measured potentials were calibrated relative to the reversible hydrogen electrode (RHE) according to the following calculation:

$$E_{RHE} = E_{Ag/AgCl} + 0.197 + 0.059pH \qquad (1)$$

The working electrodes were prepared as follows: 4 mg of the electrocatalyst was dispersed into a mixed solvent containing with ethanol and nafion (v/v=720/80) to form the homogeneous dispersion by ultrasonication treatment for 60 min. Then, 10 μL of the above solution was pipetted onto a polished glassy-carbon rotating risk electrode and dried at room temperature. The cyclic voltammetric (CV) measurements was performed in O$_2$/N$_2$-saturated 0.1 M KOH until obtaining a stable profile. Then, the linear sweep voltammetry (LSV) curves were measured to evaluate ORR or OER activity, respectively. The presented current density was normalized to the geometric surface area of electrodes. The poison

tests for ORR were performed in mixed solution containing KOH (0.1 M) and CH$_3$OH (1 M). Rotating ring disk electrode (RRDE) measurements were carried out in O$_2$-saturated KOH (0.1 M) at 1600 rpm with a scan rate of 5 mV s^{-1}, and the potential of the Pt ring was set at 1.3 V (vs RHE). The yield of H$_2$O$_2$ and the electron transfer number (n) were calculated by the following equation:

$$n = \frac{4I_D}{I_D + I_R / N} \qquad (2)$$

$$[H_2O_2]\% = \frac{200 I_R / N}{I_R / N + I_D} \qquad (3)$$

where I_D and I_R are the disk and ring currents, respectively. N is the collection coefficient at the ring in RRDE experiments (N=0.37).

A home-made aqueous rechargeable Zn-air battery were assembled with a polished Zn plate (thickness: 0.3 mm, area: 1 cm^2) as the anode, carbon paper with catalyst-coated as the air cathode, and a 6.0 M KOH + 0.2 M Zn(CH$_3$COO)$_2$·2H$_2$O mixed solution as the electrolyte. The discharge/charge cycling of rechargeable Zn-air batteries were using recurrent galvanostatic pulses for 10 min of charge followed by 10 min of discharge at 5 mA cm^{-2}. Polarization curve measurements (v-i) were performed by LSV at a scan rate of 10 mV s^{-1}. The current and power density curves were calculated from the LSV curves. All tests are performed in a natural environment.
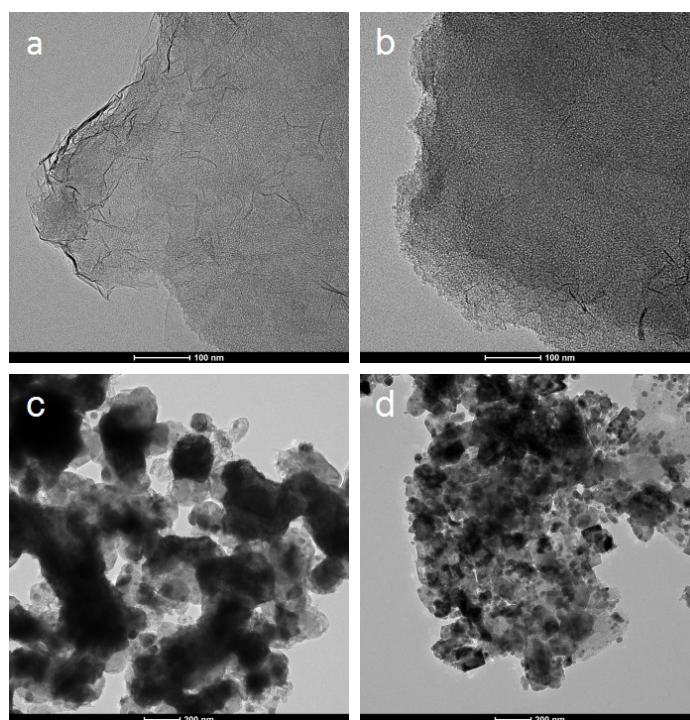
Figure S1. (a-d) TEM images of AC, NAC, Co@C-NAC and MnO-NAC
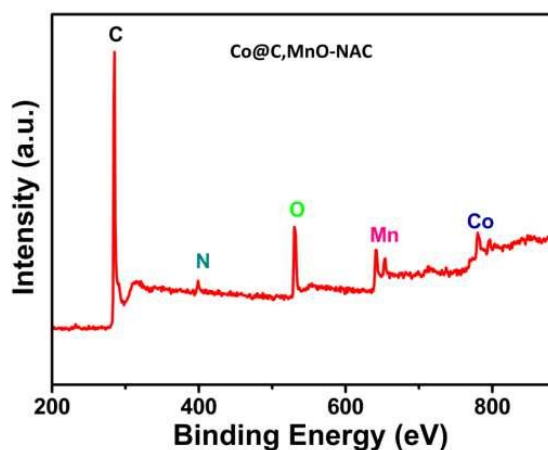
Figure S2. Survey spectrum of Co@C,MnO-NAC

Table S1. The *t*-Plot report of AC, NAC, Co@C-NAC, MnO-NAC, Co@C,MnO-NAC.

t-Plot report	S_{micro}	$S_{external}$	V_{micro}	V_{total}
	$m^2 \cdot g^{-1}$		$cm^3 \cdot g^{-1}$	
AC	452.6	1733.4	0.18	1.18
NAC	390.67	2069.60	0.15	1.33
Co@C-NAC	8.98	46.03	0.003	0.048
MnO-NAC	272.19	808.40	0.11	0.58
Co@C,MnO-NAC	234.66	838.08	0.092	0.62
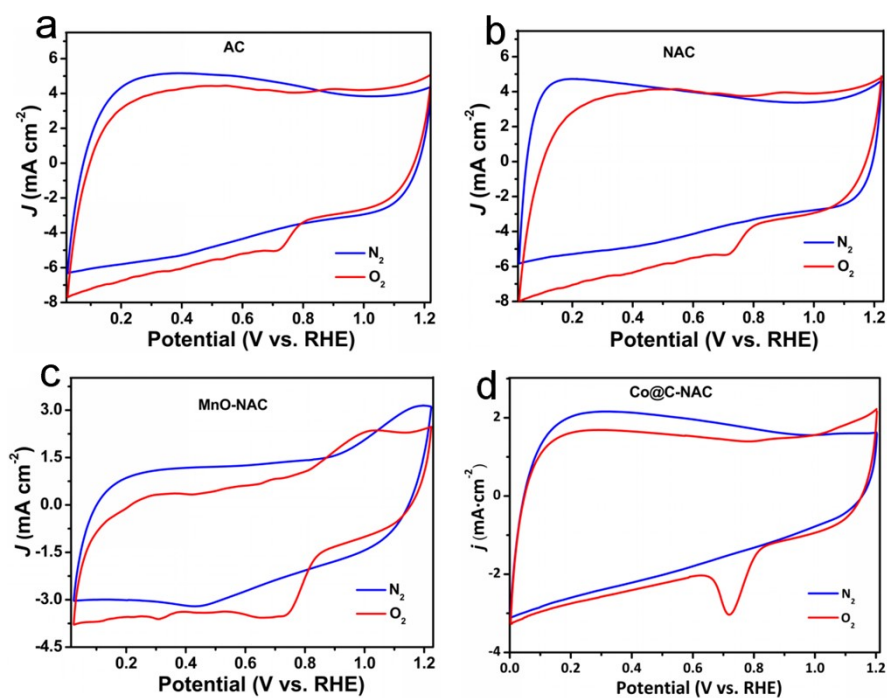
Figure S3. CVs of AC (a), NAC (b), MnO-NAC(c), Co@C-NAC(d) in O_2- or N_2- saturated 0.1 M

KOH
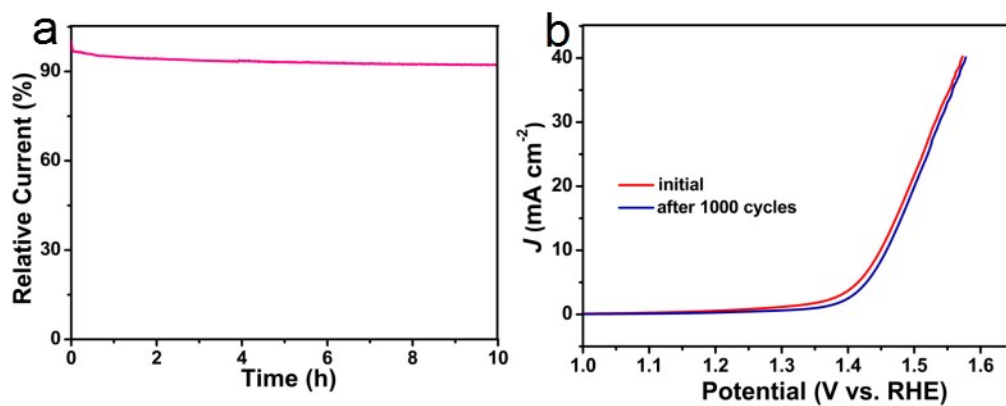
Figure S4. (a) i-t curves of Co@C,MnO-NAC performed at 1.4 V, (b) OER LSV curves for

Co@C,MnO-NAC before and after 1000 CV cycles
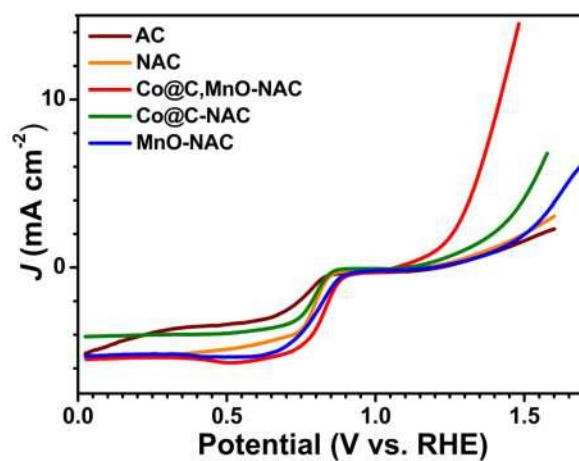
Figure S5. LSV curves of AC, NAC, Co@C-NAC, MnO-NAC, Co@C,MnO-NAC at 1800 rpm,

showing the electrocatalytic activities for ORR and OER.
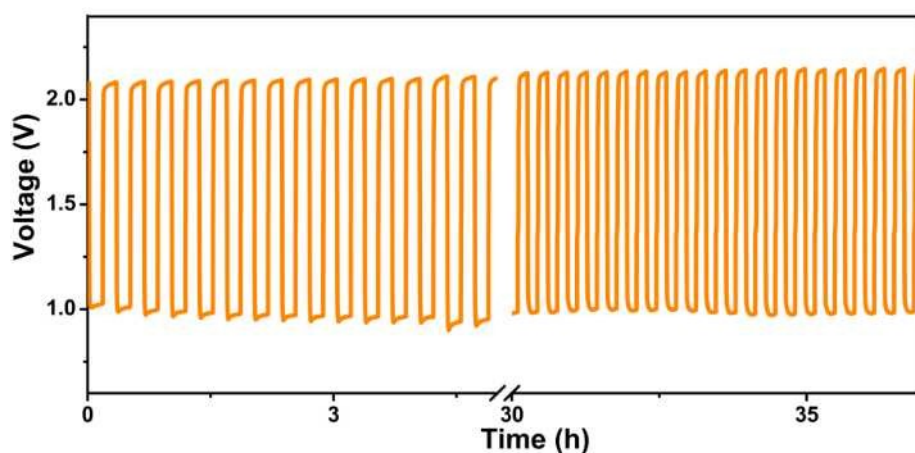
Figure S6. Galvanostatic discharge-charge cycling curves at 5 mA cm^{-2}.

Table S2 . The comparison of ORR, OER and dual catalytic performances in this work to some results from literatures.

Sample	E_{ORR} onset [V]	$E_{ORR1/2}$ [V]	Transferred electrons (*n*)	E_{OER}[V] (j=10 mA cm^{-2})	ΔE ($E_{j=10}$ - $E_{1/2}$)(V)	RZABs cycle Duration [h]	Ref.
Co/MnO/N-C	0.88	0.822	3.89	1.61	0.788	-	S1
Co@Co$_3$O$_4$/NC-1	0.90	0.80	3.78	1.65	0.85	-	S2
MnO/Co-N-G	0.89	0.82	3.89-3.98	-	-	-	S3
Co/MnO-C	0.90	0.79	3.76-3.98	1.73	0.94	11	S4
Co/MnO-C	0.906	0.819	3.89	1.61	0.791	-	S5
MnO/Co/PGC	0.95	0.78	4.0	1.537	0.757	116	S6
Co/MnO@N,S-C NT/CNFs	0.92	0.84	3.82-3.98	-	-	-	S7
Co$_3$O$_4$/Co$_2$MnO$_4$ nanocomposite	0.90	0.68	3.51–3.82	1.77	1.09	-	S8
NiCoMnO$_4$/N-rGO	0.92	0.72	3.92	1.77	1.05	-	S9
Co@C,MnO-NAC	0.92	0.83	~4.0	1.55	72	37	**This work**
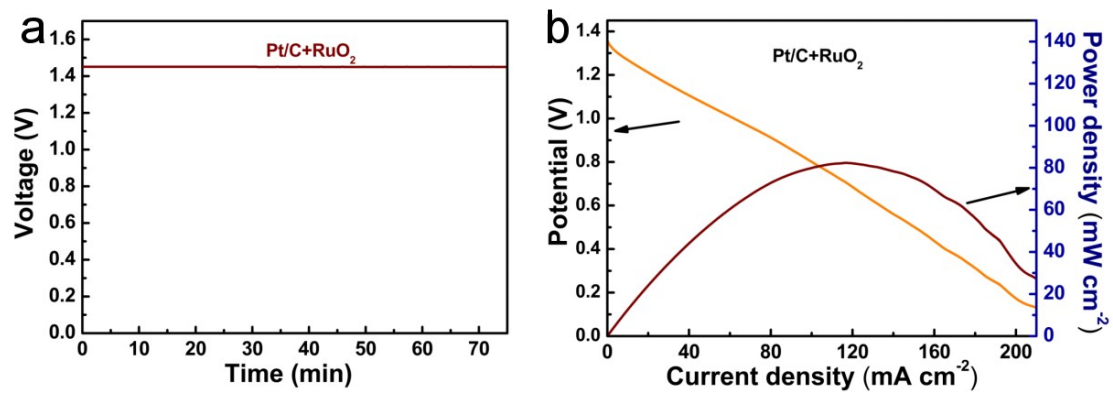
Figure S7. (a) the open-circuit potential of Pt/C+RuO$_2$, and (b) power density curves of Zn-air

battery equipped with Pt/C+RuO$_2$ as cathode material
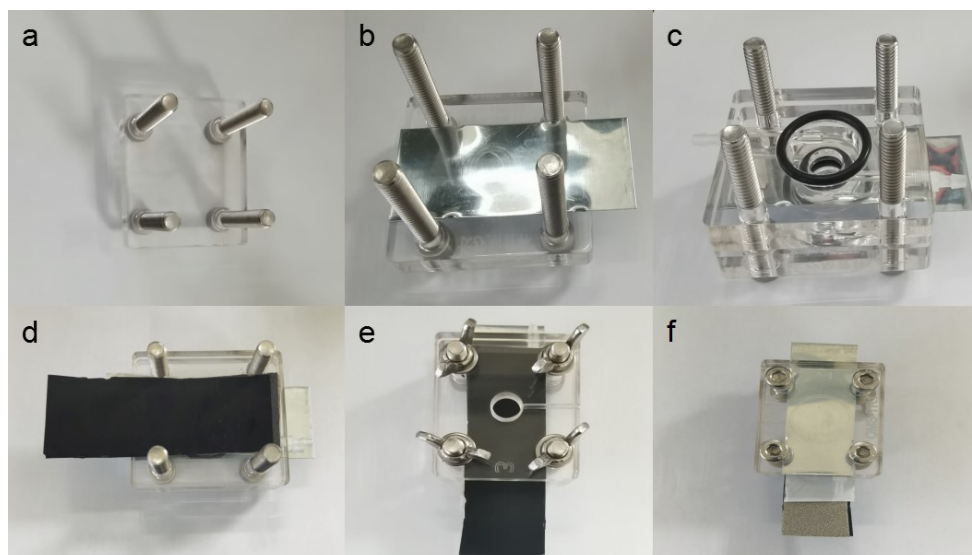
Figure S8. (a-f) Photographs of the assembly process for the fabrication of a rechargeable

Zn-air battery.
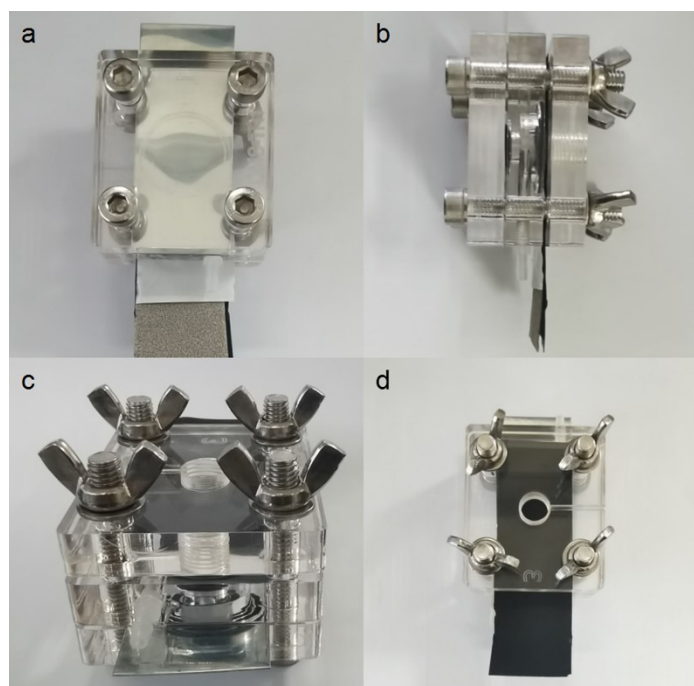
Figure S9. (a-d) Photographs of the rechargeable Zn-air battery recorded from different directions.

References:

S1: W. Wang, H. Wang, Zexing Wu b, Yang Yu, Muhammad Asif, Zhengyun Wang, Xiaoyu Qiu, Hongfang Liu. Co/MnO/N-C hybrid derived from N-methyl-D-glucamine as efficient bifunctional oxygen electrocatalysts, *Electrochim. Acta*, 2018, *281*, 486-493.

S2: A. Aijaz, J. Masa, C. Rçsler, W. Xia, P. Weide, A. Botz, R. Fischer, W. Schuhmann, M. Muhler, Co@Co$_3$O$_4$ encapsulated in carbon nanotube-grafted nitrogen-doped carbon polyhedra as an advanced bifunctional oxygen electrode, *Angew. Chem. Int. Edit.*, 2016, *55*, 4087-4091.

S3: F. Wu, Y. Niu, X. Huang, Y. Mei, X. Wu, C. Zhong, W. Hu. Manganese/cobalt bimetal nanoparticles encapsulated in nitrogen-rich graphene sheets for efficient oxygen reduction reaction electrocatalysis, *ACS Sustain. Chem. Eng.*, 2018, *6*, 10545-10551.

S4: S. Cai, R. Wang, W. Guo, H. Tang, Three-dimensional macroporous Co-embedded N-doped carbon interweaving with carbon nanotubes as excellent bifunctional catalysts for Zn–air batteries, *Langmuir*, 2018, *34*, 1992-1998.

S5: W. Wang, H. Wang, Y. Yu, Z. Wu, M. Asif, H. Liu, Metallic cobalt modified MnO-C nanocrystalline as an efficient bifunctional oxygen electrocatalyst, *Catal. Sci. Technol.*, 2018, *8*, 480-485.

S6: Xue Feng Lu, Ye Chen, Sibo Wang, Shuyan Gao, and Xiong Wen (David) Lou. Interfacing manganese oxide and cobalt in porous graphitic carbon polyhedrons boosts oxygen electrocatalysis for Zn-air batteries, *Adv. Mater.*, 2019, *31*, 1902339.

S7: Q. Zhou, S. Hou, Y. Cheng, R. Sun, W. Shen, R. Tian, J. Yang, H. Pang, L. Xu, K. Huang, Y. Tang, Interfacial engineering Co and MnO within N,S co-doped carbon hierarchical branched superstructures toward high-efficiency electrocatalytic oxygen reduction for robust Zn-air batteries, *Appl. Catal. B-Environ.*, 2021, *295*, 120281.

S8: D. Wang, X. Chen, D. Evans, W. Yang, Well-dispersed Co_3O_4/Co_2MnO_4 nanocomposites as a synergistic bifunctional catalyst for oxygen reduction and oxygen evolution reactions, *Nanoscale*, 2013, *5*, 5312-5315.

S9: A. Pendashteh, J. Palma, M. Anderson, R. Marcilla, $NiCoMnO_4$ nanoparticles on N-doped graphene: Highly efficient bifunctional electrocatalyst for oxygen reduction/evolution reactions, *Appl. Catal. B-Environ.*, 2017, *201*, 241-252.